Replacement of the Proximal Ligand of Sperm Whale Myoglobin with Free Imidazole in the Mutant His-93→Gly†

Doug Barrick

Institute of Molecular Biology, University of Oregon, Eugene, Oregon 97403

Received November 23, 1993; Revised Manuscript Received February 24, 1994®

ABSTRACT: The proximal bond between the iron atom of the heme group and the Nε of histidine F8 in myoglobin (Mb) and hemoglobin (Hb) is presumed to be an important determinant of heme binding, protein structure, and oxygen binding. Here a system is described in which the proximal ligand is provided intermolecularly by the histidine side chain mimic imidazole. The proximal ligand of sperm whale Mb is replaced with glycine (H93G) using site-directed mutagenesis. The addition of imidazole to *Escherichia coli* expressing this gene reconstitutes myoglobin function. H93G Mb purified in the presence of imidazole is spectroscopically similar to wild-type Mb in combination with a wide variety of distal ligands. The crystal structure of H93G Mb, determined in the presence of imidazole, reveals that an imidazole molecule is bonded to the heme iron on the proximal side, substituting *in trans* for the side-chain function of the proximal histidine of wild-type Mb. Although H93G Mb is similar in spectroscopic and gross structural detail to wild-type Mb, subtle differences exist in the orientation of imidazole with respect to the heme group. *trans*-Complementation of proximal ligand function will allow the proximal bond in hemoproteins to be chemically substituted beyond the limits of the genetic code.

Myoglobin and hemoglobin (Mb and Hb),[1] the vertebrate oxygen binding and transport proteins, contain heme prosthetic groups. In both of these proteins, oxygen binds directly to the iron atom of the heme at the distal site. The heme is linked to the protein through a bond between the iron atom and the invariant proximal histidine (residue 93 in sperm whale Mb). Although the structural significance of this proximal bond in Mb and Hb has long been appreciated (Kendrew, 1962; Perutz et al., 1968, 1990; Watson, 1969; Takano, 1977), a quantitative description of the role of this unique bond in heme binding, in myoglobin physiology, and in hemoglobin cooperativity is less well understood.

Model compound studies using derivatives of heme which contain a covalently attached imidazole group have shown that the binding of such a group to one side of the heme iron can increase (or decrease) by 3 orders of magnitude the affinity of oxygen or other gases in binding to the opposite side of the heme iron (Traylor & Sharma, 1992; White et al., 1979). Similar cooperative interactions are expected between the proximal and distal (gas) binding sites in the protein; however, this is currently untested. To measure this effect, it would be necessary to break and form the proximal ligand bond within the protein.

Here site-directed mutagenesis is combined with intermolecular complementation of side-chain function to produce a protein in which the proximal ligand bond can be formed and broken at will. Histidine 93, the proximal ligand in sperm whale myoglobin, is replaced with glycine (H93G). This molecular lesion is then repaired by addition of free imidazole; the intention is that free imidazole bind in the cavity left by removal of the proximal histidine and provide proximal-ligand function *in trans*. Here the function and structure of H93G sperm whale myoglobin in the presence of imidazole are examined using optical spectroscopy and X-ray crystallography.

EXPERIMENTAL PROCEDURES

The H93G mutant of the sperm whale myoglobin gene was constructed by a recombinant polymerase chain reaction (PCR) scheme (Merino et al., 1992; Barrick et al., 1993). The product of the recombinant PCR was cloned into the *Bgl*II and *Eco*RI sites of pMb413b. (pMb413b contains the synthetic gene for wild-type sperm whale Mb and is a modified version of the plasmid pMb413a, kindly provided by Drs. Barry Springer and Steven Sligar (1987).) Replacement of the codon for histidine 93 with that for glycine was confirmed by DNA sequencing using the dideoxynucleotide method (Sanger, 1981).

To measure the amount of functional myoglobin produced in *Escherichia coli*, strain TB-1 harboring the H93G Mb-bearing pMb413b was grown at 37 °C to late log phase in rich media (10 g of tryptone, 5 g of yeast extract, and 5 g of sodium chloride per liter) containing various concentrations of imidazolium chloride, pH 7.5. To 10 mL of such cultures, 50–100 mg of sodium hydrosulfite was added to reduce ferric heme to the ferrous form and scavenge molecular oxygen (Antonini & Brunori, 1971). The reduced bacterial culture was divided, and half of the sample was bubbled with carbon monoxide (CO). A difference spectrum was recorded between the deoxygenated and CO-containing samples on a Cary 118 spectrophotometer at room temperature.

To express H93G Mb for subsequent purification, imidazolium chloride, pH 7.5, was added to liquid culture media to a concentration of 10 mM. Otherwise, bacterial growth was as described (Barrick & Baldwin, 1993). Protein purification was carried out essentially as described by

† The author acknowledges support from a Howard Hughes Medical Institute Predoctoral Fellowship and a Helen Hay Whitney Postdoctoral Fellowship. This work was supported by NIH Grant GM19989 to R. L. Baldwin and by a grant from the Lucille P. Markey Foundation.

® Abstract published in *Advance ACS Abstracts,* May 1, 1994.

[1] Abbreviations: myoglobin, Mb; hemoglobin, Hb; polymerase chain reaction, PCR; carbon monoxide, CO; MbCO, ferrous myoglobin with carbon monoxide as a distal ligand; MbO_2, ferrous myoglobin with dioxygen as a distal ligand; deoxyMb, ferrous Mb without a distal ligand; MbCN, ferric myoglobin with cyanide anion as a distal ligand; metaquoMb, ferric myoglobin with water as a distal ligand.

0006-2960/94/0433-6546$04.50/0

Hughson et al. (1991), except that 1–10 mM imidazole was included in all lysis and chromatography buffers. This procedure results in approximately 5 mg of H93G Mb per liter of cell culture that is greater than 95% pure, as judged by SDS–PAGE (Laemmli, 1970).

For absorbance spectra, Mbs were diluted 100–200-fold into 0.1 M sodium phosphate, pH 7.0. To prepare deoxyMb samples, nitrogen was bubbled through the buffer solution for 5 min before sodium hydrosulfite (10 mM final), 10 mM imidazole, and Mb were added. To prepare MbCO, Mb, buffer, and sodium dithionite were bubbled with carbon monoxide for 5 min. To prepare MbO_2, Mb, buffer, and sodium hydrosulfite were bubbled with air for 5 min. Spectra were collected at room temperature using 1.00-cm quartz cuvettes, with an SLM DW-2000 dual-beam spectrophotometer. To convert absorbance values to extinction coefficients, myoglobin concentrations were measured from pyridine hemochrome spectra (Berry & Trumpower, 1987). In this method, the difference in oxidized versus reduced heme absorbance at 556 nm is measured in an alkaline pyridine solution. This difference absorbance is independent of the polypeptide and is thus well suited for concentration determination of hemoproteins in which mutationally induced spectral changes are possible.

For the X-ray crystallographic analysis, the crystal used to collect all diffraction data was grown using the hanging-drop method over a well solution containing 35% PEG 8000, 300 mM NaOAc, 0.1 M PIPES, and 0.1% dioxane, pH 6.2. Each drop was 6 mg/mL in H93G Mb and contained 5 mM imidazole. This imidazole concentration is below the estimated K_d for imidazole binding to the distal site of wild-type Mb at this pH (60–70 mM; Diven et al., 1965) and was chosen with the hope of saturating the proximal site while leaving water bound at the distal site. Crystallization appeared to be complete after 1 week. Precession photographs revealed the space group to be $P2_12_12_1$; observed cell dimensions were $a = 40.15$, $b = 49.04$, and $c = 79.14$ Å. Oscillation photographs were collected on a San Diego Multiwire systems area detector from the resolution limits 2.17–26.6 Å. Seven thousand six hundred seventy-six unique reflections were obtained in a total of 25 555 observed reflections to give a completeness of 89%. These data were combined, resulting in an R_{merge} of 3.3%. All reflections were used in subsequent Fourier synthesis and refinement, regardless of intensity.

Preliminary phases were determined by rotation and translation searches (Rossman, 1972) using a Patterson map calculated from the coordinates of wild-type sperm whale Mb (Lionetti et al., 1991) in which the side chain of His-93 and the distal ligand were omitted from the coordinates. This preliminary solution was refined using the conjugate direction method of the TNT package (Tronrud et al., 1987). Fifty-seven rounds of atomic position and temperature factor refinement yielded an R-factor of 23.3%. Calculation of an $F_{obs} - F_{calc}$ map from this partly refined model revealed a large positive lobe of electron density on the proximal side of the heme. Further refinement (140 rounds) was carried out on a model in which an imidazole molecule was built into this positive $F_{obs} - F_{calc}$ feature. During further refinement, electron density from 20 ordered water molecules could be seen in the $F_{obs} - F_{calc}$ map, and these waters were built into the model. Final refinement was made against data from 20.0 to 2.17 Å using 7171 reflections (82% completeness). The resulting model displayed deviations from ideal bond lengths of 0.021 Å, deviations from ideal bond angles of 2.9°, and a final R-factor of 17.7%.

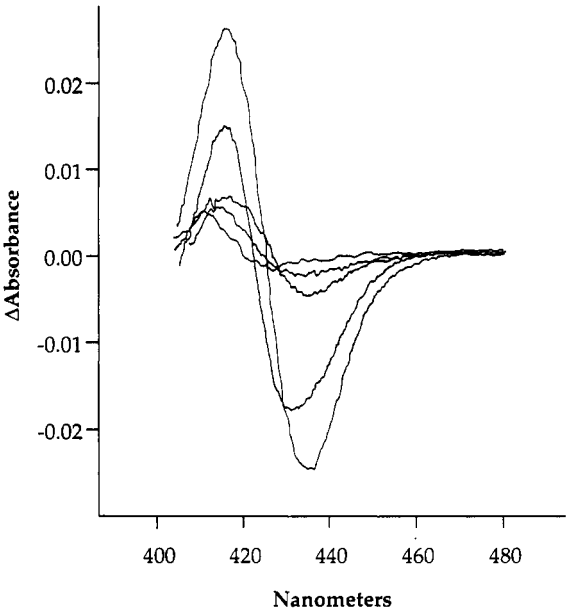

FIGURE 1: Whole-cell CO difference spectra of overnight cultures of *E. coli* harboring a plasmid encoding H93G Mb in increasing concentrations of imidazole. The difference spectrum with the greatest deflections from the baseline at 415 and 435 nm (0.051 absorbance units) was obtained from cells grown in 10 mM imidazole. Cells grown in 5 mM, 0.5 mM, or 50 μM imidazole or in the absence of imidazole show correspondingly smaller difference spectra. Spectra were recorded at room temperature at 20 nm/in, at a rate of 1 nm/s.

RESULTS

Expression of H93G Mb. The amount of functional Mb produced in *E. coli* can be determined by measuring whole-cell CO difference spectra (Springer & Sligar, 1987). This spectrum results from differences in the absorbance spectra of deoxyMb and MbCO. To determine how the amount of functional H93G Mb produced in bacterial cells depends on the addition of imidazole, cultures of *E. coli* harboring the gene encoding H93G Mb were grown in rich media containing various concentrations of imidazole. The addition of imidazole in the 0.5–10 mM range had a profound effect on the magnitude of the CO difference spectrum (Figure 1). At the highest imidazole concentrations examined, a large CO difference spectrum was observed, with a shape very similar to that obtained for cells expressing wild-type Mb in the absence of imidazole (Springer & Sligar, 1987). For cells expressing the H93G Mb gene in the absence of imidazole, however, the CO difference spectrum is comparatively featureless (Figure 1). Since this difference spectrum is sensitive both to proper distal ligand binding and to the spectral features resulting from binding of these distal ligands, the results suggest that the addition of imidazole to H93G Mb produces a functional protein with spectroscopic features similar to those of wild-type Mb.

Absorbance Spectroscopy of H93G Mb. To investigate further the distal ligand specificities and associated spectral properties of H93G Mb complexed with imidazole, H93G Mb protein was purified to homogeneity in the presence of imidazole. Absorbance spectroscopy in the ultraviolet and visible ranges of various distal ligand derivatives shows similar spectral features for wild-type and H93G Mbs, for both the ferrous (Figure 2; Table 1) and the ferric (Figure 3; Table 2) forms of the protein. In Figures 2 and 3, absorbance values are reported as millimolar extinction coefficients (see Experimental Procedures); spectra above 470 nm are multiplied by 8 to allow a detailed examination of spectral shape.

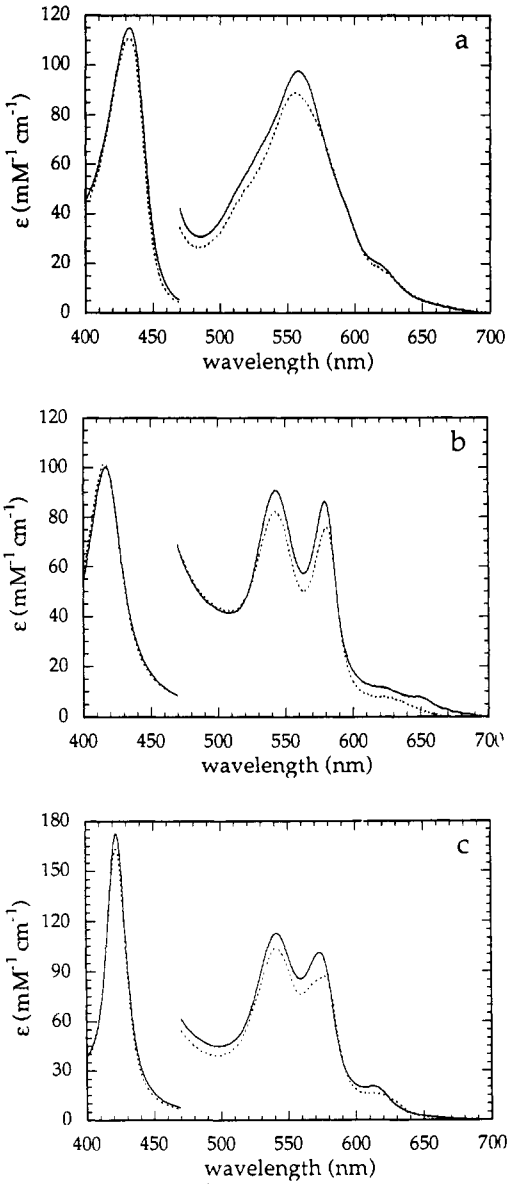

FIGURE 2: Absorbance spectra of H93G (—) and wild-type (- - -) ferrous Mbs: (a) deoxyMb, (b) Mb·O_2, and (c) Mb·CO. Samples were prepared as described in the text and contained 10 mM imidazole. Data at 470 nm and above are scaled by a factor of 8 to allow comparison of the less intense visible bands.

For the ferrous forms of the protein, H93G deoxyMb shows a Soret peak centered at 432.5 nm. This peak is quite similar to that of wild-type deoxyMb in shape, magnitude, and position. Similarities are also seen for both H93G and wild-type deoxyMb in the visible region (from 500 to 700 nm), although a slight (2 nm) blue shift is obtained for the absorbance maximum of wild-type Mb (Figure 2A; Table 1). Addition of O_2 results in similar spectral changes for H93G and wild-type Mb (Figure 2B; Table 1). In particular, the addition of O_2 causes a 10–12-nm blue shift of the Soret band for both proteins. Furthermore, the single peak seen in the visible region of the deoxy spectrum for both proteins is split into two bands. Similar splitting of this peak is also observed upon addition of CO for both H93G and wild-type Mb. The addition of CO also produces similar changes in the Soret bands of H93G and wild-type Mb (Figure 2C, Table 1): for both proteins the Soret band sharpens substantially and shifts to 422.5 nm.

Ferric H93G and wild-type Mb also show similar absorbance spectra in the presence of various potential distal ligands,

Table 1: Absorbance Maxima of Ferrous (Fe^{2+}) Wild-Type and H93G Myoglobins[a]

protein	absorbance maxima (nm)		
	Soret	β[b]	α[b]
deoxyMb			
H93G	432.5	557.5	
wild type	432.5	555.5	
MbCO			
H93G	422.5	541	572.5–574
wild type	422.5	541.5	576.8
MbO_2			
H93G	416.5–417	543	578–579
wild type	415.8	542	580–581

[a] Samples contained, in addition to 3–6 μM Mb and 10 mM imidazole, 0.1 M sodium phosphate, pH 7.0; spectra were obtained at 25 °C. [b] Visible bands are named according to the convention used by Antonini and Brunori (1971).

although the preparation of the metaquoMb derivative (with water bound as a distal ligand) in H93G is complicated by the ability of imidazole to bind as a distal ligand in the ferric form (Antonini & Brunori, 1971; Scheler et al., 1957; Lionetti et al., 1991). For wild-type Mb, imidazole binds with a K_d around 30 mM at pH 7.0 (Diven et al., 1965). Indeed, at high imidazole concentrations (0.2 M) the spectra of H93G and wild-type Mb are very similar (Figure 3B; Table 1): the positions of the Soret bands are 415.5 and 414–414.5 nm for H93G and wild-type Mb, respectively, while in the visible region, peaks centered at 533.5 nm are seen for both proteins, with shoulders between 560 and 565 nm. These values are very similar to published data for wild-type Mb with distally bound imidazole (Scheler et al., 1957; Diven et al., 1965). Lower concentrations of imidazole (0.2 mM) produce similar spectroscopic changes for ferric H93G and wild-type Mb (Figure 3A; Table 1), and at 0.2 mM imidazole both spectra closely resemble the published spectral values for metaquoMb (Antonini & Brunori, 1971). Although the absorbance spectrum of wild-type myoglobin is not affected by a further decrease in imidazole concentration, the absorbance spectrum of H93G shows a significant imidazole dependence below 0.2 mM (not shown). It is possible that these changes result from dissociation of imidazole from the proximal ligand site. The addition of 10 mM KCN to H93G and wild-type Mb samples containing 0.2 mM imidazole produces similar spectral changes (Figure 3C; Table 1). Soret bands shift to 422.5 nm for both proteins, the visible bands for both proteins change shape and shift to 538 nm for both proteins, and bands in the near-UV region (358 and 358.5–359 nm for H93G and wild-type Mb) appear. These spectral features are very similar to those reported for sperm whale MbCN (Antonini & Brunori, 1971).

X-ray Structure Determination. To confirm that imidazole is acting as a proximal ligand in H93G Mb, a high-resolution crystal structure of the H93G metaquoMb variant was determined in the presence of imidazole. Using a model with glycine at position 93 and lacking proximal and distal ligands during refinement led to a large, clear lobe of electron density attached to the heme iron on the proximal side which was not accounted for by the model. On the distal side of the heme, a much smaller lobe of electron density was seen. For further refinement an imidazole molecule was built into this extra proximal density. In addition the locations of 20 water molecules were inferred from the electron density, including what appeared to be a single water molecule on the distal side of the heme, and these waters were built into the model. Further refinement of the model against data from 20.0 to 2.17 Å gave an overall R-factor of 17.7%.

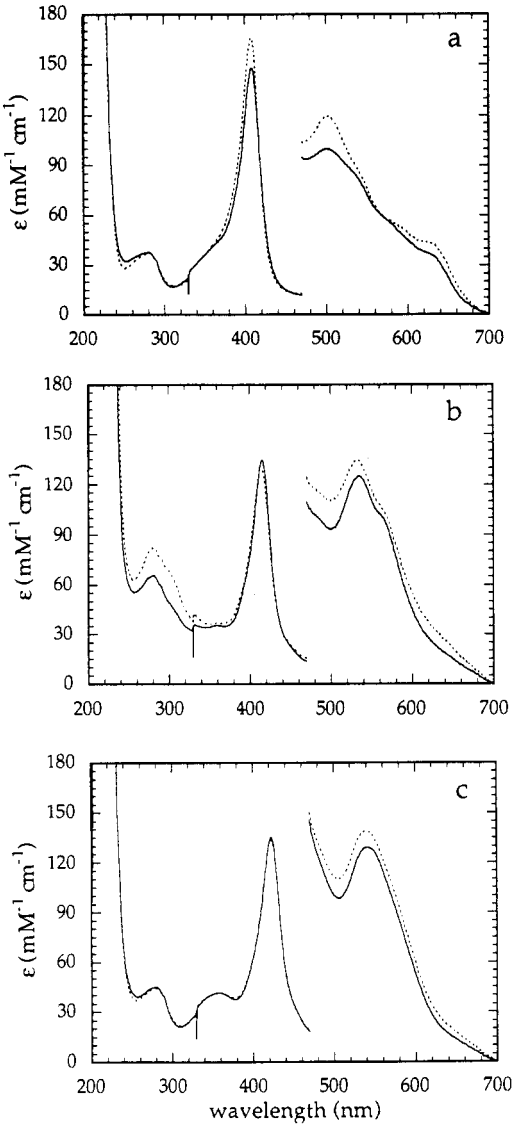

FIGURE 3: Absorbance spectra of H93G (—) and wild-type (- - -) ferric Mbs: (a) metaquoMb, (b) Mb with high (0.2 M) concentrations of imidazole, and (c) Mb·CN. Samples were prepared as described in the text. Data at 470 nm and above are scaled by a factor of 8 to allow comparison of the less intense visible bands.

The heme, the proximal imidazole molecule, and several neighboring residues from this final model are shown in Figure 4. The electron density (or omit map) is an $F_{obs} - F_{calc}$ map contoured at 4σ calculated from the final model from which the imidazole molecule has been removed.[2] As can be seen in Figure 4, the position of the proximal imidazole in the final model is clearly defined by this electron density. Comparison of panels a and b of Figure 4, which are face-on and edge-on views of the same structure, shows the electron density to be asymmetric with respect to the heme normal, restricting the orientation of the imidazole plane about this normal to that shown. Furthermore, the average of the thermal factors for the five imidazole atoms (32 Å^2) is similar to those for the histidine side chains in the model, including the distal histidine (His-64) and the neighboring His-97, suggesting that the imidazole is well ordered. Further discussion of the degree to which the electron density supports the orientation of the imidazole shown in Figure 4 is reserved for the Discussion section.

[2] Prior to calculation of the omit map, a further 10 cycles of refinement were carried out to allow relaxations in the omit model.

Table 2: Absorbance Maxima of ferric (Fe^{3+}) Wild-Type and H93G Myoglobins[a]

protein	absorbance maxima (nm) δ[b]	Soret	visible	CT[b]
metaquoMb				
H93G		408.5–409	498.5–505	~630[c]
wild type		408	502–503.5	~630[c]
Mb + 0.2 M imidazole				
H93G		415.5	535.5, 560–565[c]	
wild type		414–415.5	535.5, 560–565[c]	
MbCN				
H93G	358	422.5	538	
wild type	358.5–359	422.5	537.5–538	

[a] Samples contained 0.2 mM imidazole, except where noted, in which case the concentration of imidazole was 0.2 M. MbCN samples contained 10 mM KCN. In addition, all samples contained 3–6 μM Mb and 0.1 M sodium phosphate, pH 7.0; spectra were obtained at 25 °C. [b] The δ and CT (charge transfer) bands are named according to the convention used by Antonini and Brunori (1971). [c] The metaquoMb CT bands and the Mb + 0.2 M imidazole visible bands are shoulders; therefore, estimated absorbance maxima are subject to considerable uncertainty.

In the orientation shown in Figure 4, the imidazole is well separated from Gly-93, the residue which in wild-type Mb provides the proximal ligand to the heme iron. The distance between the methine carbon of imidazole most equivalent to the Cγ of His-93 in wild-type Mb (the upper right carbon of imidazole in Figure 4a, C(5)[3]) and the Cα of Gly-93 is 4.2 Å; the equivalent distance in wild-type Mb is 2.5 Å. Other significant features of the environment surrounding the proximal imidazole are the proximity of the hydroxyl group of Ser-92 to the imino (nonliganded, N_i) nitrogen of imidazole: these two groups are separated by 2.7 Å and appear to be in a good geometry for hydrogen bonding. Furthermore, one of the propionate carboxylates from the heme is in a similar orientation: the distance between one of its two carboxylate oxygens and the imidazole imino nitrogen is 3.3 Å.

The orientation of the imidazole molecule with respect to the heme iron and the porphyrin skeleton is shown in Figure 5. Geometric parameters describing the relative orientation of heme and imidazole, as defined in Figure 6, are listed in Table 3. Mean planes for heme and imidazole were calculated using the program edpdb (Zhang, 1992). The distance from the heme iron to the tertiary (liganding, N_t) nitrogen of imidazole is 1.9 Å. The angle between the iron to imidazole N_t bond and the heme normal (θ) is 2.5°. The angle between the iron to imidazole N_t bond and the imidazole plane (χ) is 13.8°.[4] A discussion of the significance of these values and a comparison to the structure of wild-type Mb are reserved for the Discussion section.

DISCUSSION

Axial ligands in heme proteins have long been recognized as important for both structure and function in heme proteins (Kendrew, 1962; Watson, 1968; Perutz, 1969, 1990; Dunford

[3] The nomenclature used to describe the imidazole ring is consistent with IUPAC conventions (Reynolds et al., 1973; Hoffman, 1953), in which numbering proceeds from the imino nitrogen (the nitrogen bound to a hydrogen atom in the deprotonated form, termed N_i,) toward the tertiary nitrogen (termed N_t). This nomenclature is related to the usual protein designations as follows: Cγ = C(5); Nδ1 = N(1) = N_i; Cε1 = C(2); Nε2 = N(3) = N_t; Cδ2 = C(4).

[4] The angle between the heme and imidazole planes (Ω) is 75°. Although on the basis of the two-dimensional representation of Figure 6 it appears that the sum of χ, θ, and Ω should be 90°, the three-dimensional rotation of the imidazole about the iron-to-imidazole N_t, i.e., rotation about ϕ (the dihedral angle in which the iron-to-N_t bond is the central bond) invalidates this equality.

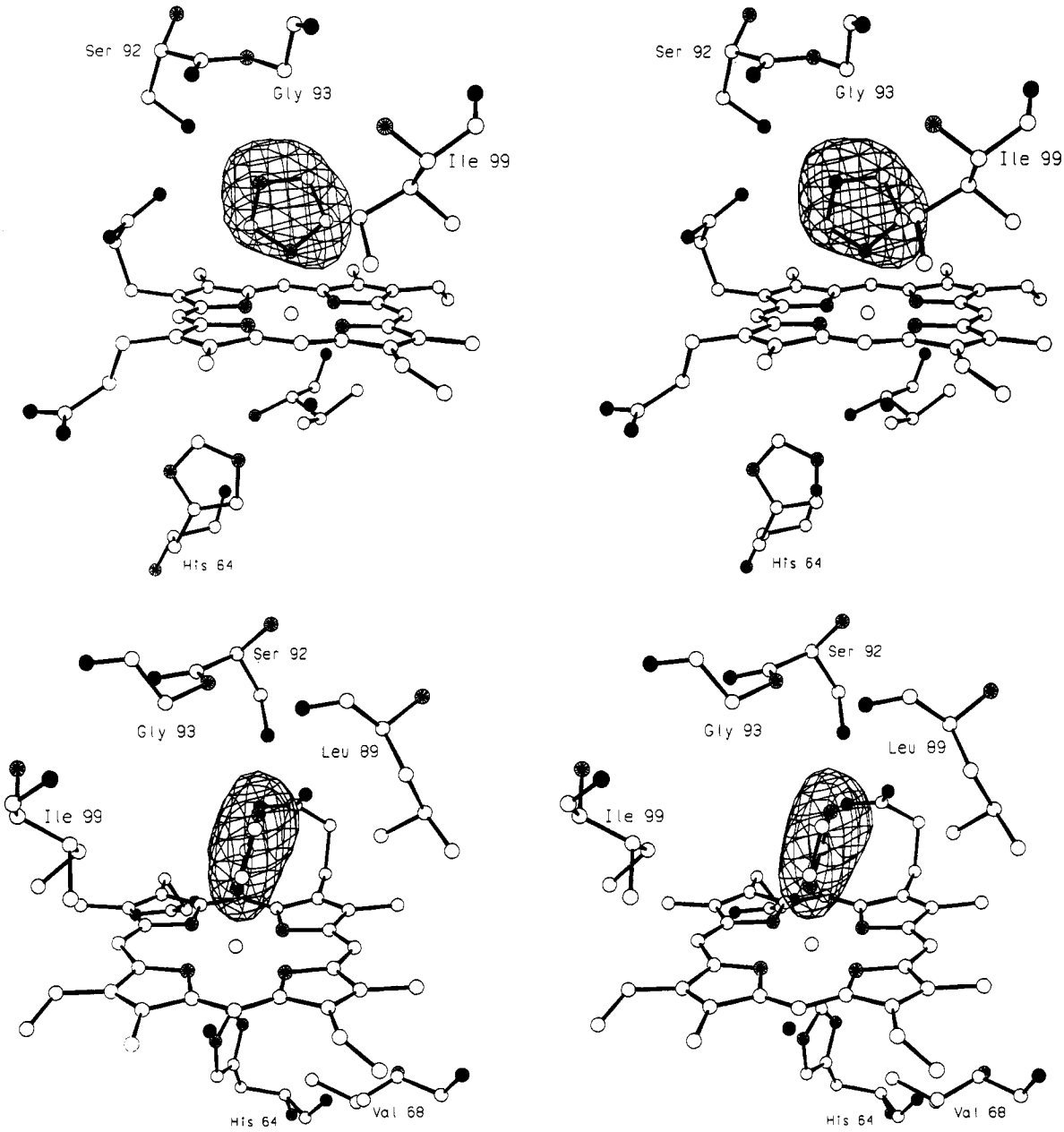

FIGURE 4: Omit maps of the heme, the imidazole, and the surrounding region of H93G Mb. The model is the result of refinement with imidazole as shown. The electron density is from an $F_{obs} - F_{calc}$ map contoured at 4σ which was calculated from a model lacking the imidazole molecule (see text). The imidazole molecule, in its refined position, is well bounded by the extra density in the omit map. (a, top) Stereo image of the H93G Mb heme region perpendicular to the imidazole plane. (b, bottom) Stereo image of the H93G Mb heme region parallel to the imidazole plane. Carbons are shown as open spheres; oxygens, as solid spheres; and nitrogens, as radially spoked spheres. The heme iron is also shown as an open sphere.

& Stillman, 1976; Ortiz de Montellano, 1986). In these hemoproteins, one or both ligands are residues from within the protein. These residues, usually histidine (myoglobin, hemoglobin, cytochromes *b* and *c*), tyrosine (catalase), cysteine (cytochrome P-450, chloroperoxidase), or methionine (cytochrome *c*), all share the ability to act as Lewis bases, donating electrons into empty orbitals on the iron. With the advances in site-directed mutagenesis and recombinant DNA technology over the last decade and a half, it has become possible to replace an axial ligand with another of the 20 naturally occurring amino acids. In sperm whale myoglobin, replacement of the proximal histidine with the basic residues tyrosine (Egeberg et al., 1990; Adachi, 1991, 1993) and cysteine (Adachi et al., 1991, 1993) results in changes in spectroscopic as well as functional properties. In cytochrome *c*, the replacement of an axial methionine with histidine produces a bis(histidine) (cytochrome b_5) hemoprotein (Raphael & Gray, 1989), while replacement with alanine produces an oxygen-binding hemoprotein with spectroscopic properties similar in some respects to those of myoglobin (Bren & Gray, 1993). Here a different strategy is adopted. The proximal histidine of sperm whale Mb is replaced by glycine, a residue which lacks a side chain. The rationale is that, by clearing the region around the proximal site with this extreme truncation (H93G), small basic molecules will be able to bind and serve as proximal ligands *in trans*. In this report, data are presented for the interaction of imidazole, a close mimic of the histidine side chain, with H93G Mb. Although small changes are observed in both the crystal structure and the absorbance spectra, the overall result is clear: imidazole can function as a proximal ligand in H93G Mb, and its overall structure and function are very similar to those of His-93 of wild-type Mb.

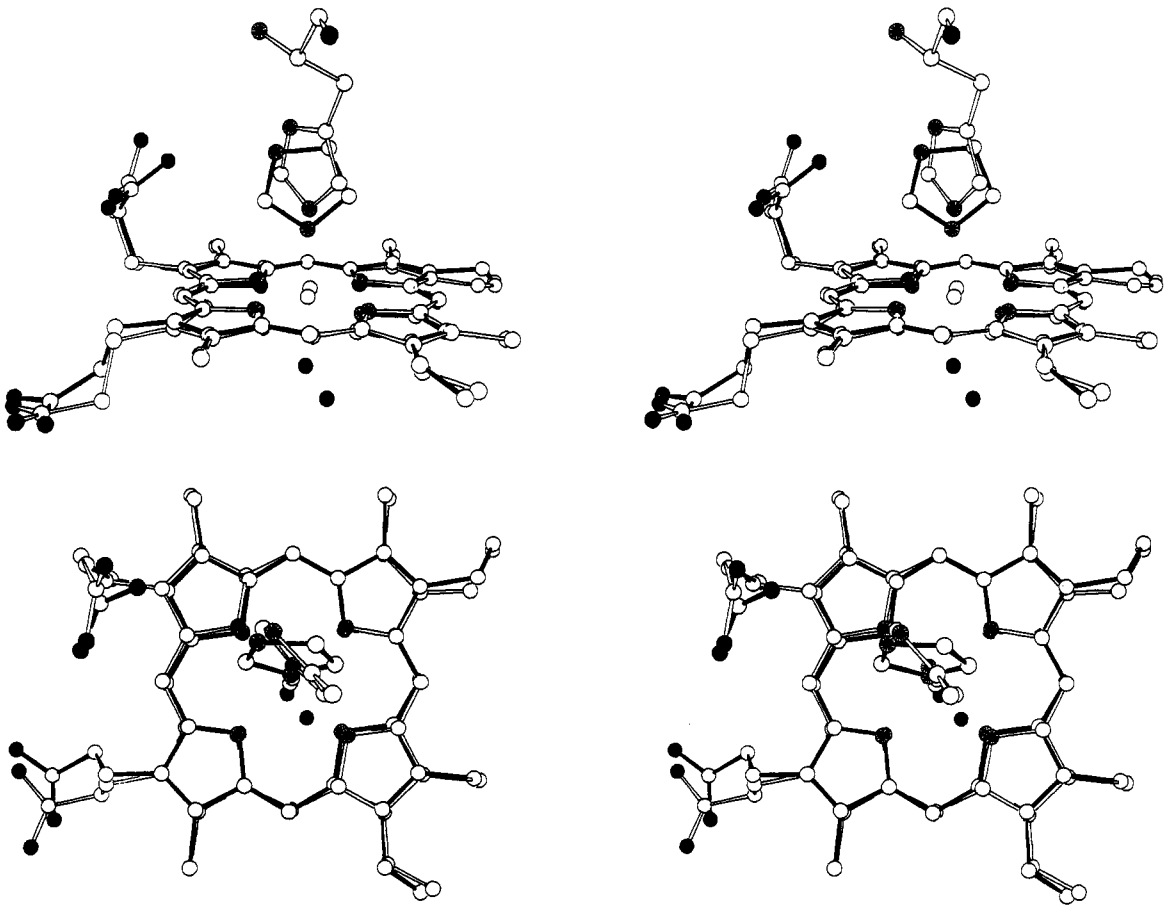

FIGURE 5: Comparison of the stereochemistry of the heme–proximal ligand interaction of H93G (solid bonds) with that of wild-type Mb (open bonds). The wild-type structure is from Takano (1977). The structures are aligned using the 20 pyrrole and 4 bridging methine atoms of the heme (see text). Atom types are represented as in Figure 4. (a, top) Stereo image from the side of the hemes. (b, bottom) Stereo image from above the hemes. The water molecule belonging to the H93G structure is the lower right black sphere in (a) and the black sphere nearest the lower right heme pyrrole nitrogen in (b).

Combination with Distal Ligands. The spectra presented in Figures 2 and 3 show that the absorbance spectrum of H93G, in the presence of imidazole, is very sensitive to the addition of various distal ligands (CN^- and high concentrations of imidazole for the ferric form, and CO and O_2 for the ferrous). These changes are very similar to those of the spectra of wild-type Mb when presented with the same range of distal ligands and are indicative of distal ligand binding in wild-type Mb. Thus, the spectral changes produced by the addition of these ligands to H93G are taken as evidence that these ligands are binding to H93G Mb in a mode similar to that seen for wild-type Mb, i.e., as distal ligands. Although this assertion lacks structural proof for most ligands, in the crystal structure presented here (ferric H93G metaquoMb) the expected ligand arrangement is confirmed: an imidazole molecule is bound on the proximal side of the heme, and a water is bound on the distal side.

Comparison of Visible Spectra of H93G with Imidazole to Those of Other Mb Axial Ligand Substitutions. As shown above (Figures 2 and 3; Tables 1 and 2), the visible and UV absorbance spectra of H93G Mb, in the presence of imidazole, are very similar to those of wild-type Mb. Here this similarity is contrasted with the relatively large differences in the absorbance spectra of sperm whale Mb proximal ligand mutants in which His-93 is replaced by either Tyr (H93Y; Egeberg et al., 1990; Adachi et al., 1991, 1993) or Cys (H93C; Adachi et al., 1991, 1993). For metaquoMb, large changes in both the Soret and visible bands result from substitution with Cys and Tyr. Although the Soret band moves by only 0.5–1.0 nm for H93G relative to that of wild-type metaquoMb (0.2 mM imidazole; Table 2, Figure 3a), for H93Y and H93C it is blue shifted by 6 and 17 nm, respectively. The visible band at 502–503 nm in wild type, which, although diminished in intensity in H93G, is located at approximately the same wavelength, is blue shifted by over 20 nm for H93Y. Furthermore, the charge-transfer band, which in the spectra of wild-type Mb and H93G metaquoMb appears as a shoulder around 630 nm, is shifted to 598 nm for H93Y metaquoMb (Egeberg et al., 1990; Adachi et al., 1991, 1993). Large differences also exist between the absorbance spectra of the ferrous forms of wild-type Mb and H93G metaquoMb, and those of H93Y and H93C. While Soret bands of the wild-type and H93G deoxyMbs are both centered at 432.5 nm, they have shifted to 428 nm for the H93Y and H93C deoxyMbs (Egeberg et al., 1990; Adachi et al., 1991, 1993). Similar, albeit smaller, shifts are seen for both the Soret and visible bands of the CO derivatives of H93Y and H93C Mb. The Soret peaks of H93Y and H93C are centered at 418 and 420 nm, respectively (Egeberg et al., 1990; Adachi et al., 1991, 1993), compared with those of wild-type and H93G Mb, both of which are located at 422.5 nm. The similarity of absorbance spectra of various ligand complexes suggests that the electronic structure surrounding the heme in H93G Mb is quite similar to that in wild-type Mb. Furthermore, the observation that different distal ligands, each of which produces a unique absorbance spectrum when bound to Mb, produce similar spectra for H93G and wild-type Mb in the presence of

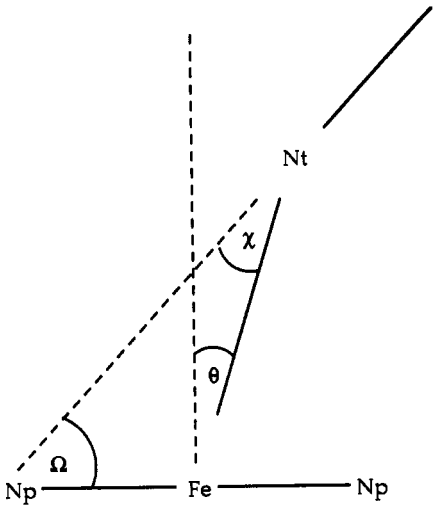

FIGURE 6: Bond and dihedral angles between the proximal imidazole and the heme. The heme plane is schematized as the horizontal line segments connecting the iron (Fe) to the heme pyrrole nitrogens (Np, only two of which are shown). The heme normal is schematized by the vertical dashed line intersecting the Fe atom. The imidazole plane is schematized by oblique line extending up from the N_t (upper right); the dashed line from the N_t is an extension of this plane. Ω is the dihedral angle between the heme and imidazole planes, θ is the angle between the heme normal and the Fe to N_t bond, and χ is the angle between the Fe to N_t bond and the imidazole plane.

imidazole suggests that these two proteins interact with these different distal ligands in similar ways.

Crystal Structure of H93G Mb with Imidazole Bound. Determination of the structure of ferric H93G Mb in the presence of imidazole by X-ray crystallography demonstrates that, for H93G Mb, imidazole functions as a proximal ligand *in trans*. The crystallographically observed preference of imidazole for the proximal site may result in part from proximal stabilization through the hydrogen-bonding interactions seen between the imidazole N_t and the Ser-92 hydroxyl and propionate carboxylate groups (Figure 4; Table 3). In addition, the binding of imidazole to the distal site in wild-type myoglobin has been observed to be weak (Diven et al., 1965), and its binding induces substantial rearrangement of distal residues, in particular of His-64 (Lionetti et al., 1991). This rearrangement is not seen in H93G Mb; the orientation of the side chain of His-64 in H93G is similar to that in wild-type Mb, and this side chain would clash severely with an imidazole molecule binding on the distal face of the heme. Although the structure of H93G ferric metaquoMb is similar to that of wild-type Mb in that the proximal ligand is provided by an imidazole ring, subtle differences in the stereochemistry of the heme–proximal ligand interaction are seen. These differences are described below; however, such a description requires that the position of the imidazole molecule in H93G Mb is correctly determined.

Orientation of the Imidazole Molecule. Although the orientation of the imidazole is well defined with respect to rotation about the heme normal by the density (the asymmetry in the omit map (Figure 4) defines the imidazole plane), the orientation of the imidazole about its own normal, that is, within the imidazole plane, is not well determined by the electron density. Nonetheless, the orientation shown in Figure 4 seems reasonable, on the basis of the position of the atoms making up the proximal cavity. In particular, it seems very likely that the basic imidazole N_t (rather than the protonated N_i) forms the proximal bond to the heme iron. This restriction limits the orientation of the imidazole to two possible

Table 3: Stereochemistry of the Heme–Axial Ligand Interaction in H93G and Wild-Type Myoglobin

	H93G[a]	wild type[b]
distance (Å)		
N_t to Fe^{3+} [c]	1.9	2.2
N_t to heme plane	1.9	2.4
Fe^{3+} to heme plane	0.03	0.23
Fe^{3+} to distal water	2.7	2.1
distal water to His-64 Nε2	2.7	2.6
Ser-92 Oγ to proximal N_t[e]	2.7	2.9
Res-93 Cα to C(5)[d]	4.2	2.5
heme propionate Oγ to proximal N_t[e]	3.3	4.5
angle (deg)		
θ	2.5	2.3
χ	13.8	0.8
Ω	75	87.4
ϕ_1, ϕ_2[e]	35, 52	−3, −1

[a] From this study. [b] From the sperm whale metaquoMb structure of Takano (1977). [c] N_t and N_i refer to the tertiary and imino nitrogens of the proximal ligand, respectively (see footnote 2); N_t is defined as the nitrogen that is bonded to the heme iron. [d] Refers to the Cα's of Gly-93 and His-93 for H93G and wild type, respectively; the C(5) position is equivilant to the Cγ of His-93. [e] ϕ_1 and ϕ_2 refer to the dihedral angles about the Fe^{3+} to imidazole N_t bond, with ϕ_1 being from imidazole C(2) to imidazole N_t to Fe^{3+} to Np_a, and ϕ_2 being from imidazole C(4) to imidazole N_t to Fe^{3+} to NP_c.

positions: the one shown in Figure 4 and one in which the imidazole is flipped 180° within its plane. The orientation in Figure 4 is likely to be favored, since it places the N_t (Figure 4a, upper left) within hydrogen-bonding distance of both the Ser-92 hydroxyl and the carboxylate of the heme propionate. Either of these groups could act as a hydrogen bond acceptor to the N_i, which is assumed to be protonated. In the alternate conformation (not shown) these two hydrogen-bonding groups are placed next to an imidazole methine (C(5)), and the N_t is in an environment which lacks hydrogen bond acceptors. Furthermore, the orientation shown in Figure 4 is similar to that of the His-93 side chain of wild-type myoglobin with respect to the positioning of the N_t and C(5).

Comparison to the Wild-Type Structure. To aid in comparing the stereochemistry of heme–axial ligand interactions between the H93G and wild-type Mb structures, the two structures were aligned (Figure 6) by minimizing the sum of the square of distances between corresponding atoms of the wild-type and H93G heme skeletons in both structures (20 pyrrole and 4 bridging methine atoms), using the algorithm of Mclaughlan (1979) implemented in the program edpdb (Zhang, 1992). One difference between the H93G and wild-type Mb structures is the distance between the hemes and respective axial ligands. Compared with that of wild-type Mb, the proximal ligand (N_t) to iron distance has shortened by 0.3 Å (Figure 5a; Table 3). This shift of the proximal imidazole is even larger (0.5 Å) if the distance is measured from the proximal N_t to the heme plane (Table 3).

In addition to a decreased distance between the heme and the proximal imidazole for H93G Mb, two distinct rotations of the imidazole are seen. First, the angle between the planes of the heme and the imidazole (defined by Ω in Figure 6) is decreased from 87.5° in wild-type Mb to 75° in H93G Mb (see Figure 5a and Table 3). This tilting may permit more favorable interactions between imidazole N_t and the neighboring polar groups. Second, there is a rotation of the imidazole about the Fe–N_t bond (Figure 5b); this can be described as changes in dihedral angles (ϕ's) as defined in footnote *e* of Table 3. When these angles are 0° or 90°, the C(2) and C(4) atoms eclipse the pyrrole nitrogens, and steric repulsions between these atoms are expected (Collins et al.,

1972; Hoard, 1975); this strain should be relieved either by increasing these angles (ϕ's) to ±45° or by increasing the distance between the ligand and the heme plane (Fe–N_ϵ bond length). As defined in footnote *e* of Table 3, these two angles increase from −1° and −3° in wild-type Mb to 35° and 52° in H93G Mb; these new values are expected to relieve the strain produced between the imidazole C(2)/C(4) and heme Nps[5].

The rotation of the imidazole about the Fe–N_ϵ bond to more favorable values of ϕ in H93G Mb and the 0.5-Å decrease in the distance between the imidazole and the heme are likely to be correlated; correlation between bond length and favorable values of ϕ has been seen in the crystal structure of a bis-(imidazole) complex of $\alpha,\beta,\gamma,\delta$-tetraphenylporphinatoiron-(III) chloride (Collins et al., 1972). Although it is not possible to tell whether the tendency to form a shorter bond drives the ϕ rotation or the ϕ rotation is brought about by other factors and closer approach of the imidazole to the heme is an indirect consequence,[6] it appears that in the wild-type Mb the attachment of the proximal histidine side chain prevents the closer approach, the favorable ϕ rotation, or both. In other words, the polypeptide architecture prevents optimal proximal ligand interactions from occurring in wild-type sperm whale metaquoMb. This is supported by the observation that the distance between the imidazole C(5) and the Cα of Gly-93 is 4.2 Å. In wild-type Mb this distance is 2.5 Å (Takano, 1977), and it does not appear that the His-93 side chain could be placed in an orientation similar to that seen in H93G without substantial repositioning of the polypeptide.

Two other differences in the heme–axial ligand stereochemistry are observed between H93G and wild-type Mb. First, the distance of the iron from the heme plane in wild-type Mb is 0.23 Å (Takano, 1977), while in the H93G structure the iron is nearly in the plane (Table 3). Positioning of the iron within the heme plane is not expected, as in this oxidation state and liganding arrangement the iron is expected to be high spin, should have a larger radius (Pauling, 1960), and should fit poorly into the plane (Hoard, 1968; Perutz, 1970). One possible explanation is that the out of plane displacement seen in wild-type metaquoMb (0.23 Å toward the proximal histidine) results in part from pulling of the iron by the proximal histidine; this pull is not expected for the free imidazole ligand in H93G. This is consistent with the lengthening of the proximal N_ϵ to iron bond in wild-type Mb (Table 3). Another possibility is that subtle changes in stereochemistry and electronic structure in the imidazole–H93G complex influence the spin state of the iron. A third possibility is that this modest difference in iron position results from crystallographic error.

A second change in the heme–axial ligand stereochemistry is an increased distance (by 0.6 Å) between the iron and the distal water in H93G Mb (Figure 5; Table 3). This increased distance results from a shift of the distal water both down (Figure 5a) and away from (Figure 5b) the heme center. Although this distance has increased, the distance between the distal water and the Nϵ2 of His-64 (the distal histidine) is the same within error (Table 3).

In summary, on the basis of the structural and spectroscopic data presented above, it is concluded that free imidazole can act both structurally and functionally as a proximal ligand *in trans* in the H93G variant of sperm whale Mb. The method described here for intermolecular complementation of the proximal ligand of Mb can be used to determine the strength of the proximal ligand bond, and the effect of this bond on the binding and release of distal ligands such as molecular oxygen, the origin of cooperativity in hemoglobin. Furthermore, combination of H93G with various other ligands will allow a detailed analysis of heme ligand chemistry, should help in understanding mechanism and function in heme-based enzymes such as cytochrome P-450 and catalase (Ortiz de Montellano, 1986; Dunford & Stillman, 1976), and may yield molecules with synthetically useful epoxidation properties (Collman et al., 1993). In addition, this method will serve as a valuable tool for the study of metalloproteins in general and may be exploited to modulate protein function both *in vitro*, as has recently been demonstrated in the copper-binding site of azurin (den Blaauwen & Canters, 1993), and *in vivo*.

[5] Note that since in H93G Mb the plane of the imidazole is also tilted away from the heme normal by 15° (90° − Ω), the values of ϕ_1 and ϕ_2 differ from each other by the degree to which the C(2)–N_ϵ–C(4) bond angle is projected onto the heme plane. In fact, the values ϕ_1 = 35° and ϕ_2 = 52° also imply that ϕ_3 = 55° and ϕ_4 = 38°. Although for an axial ligand with a 90° Ω angle both C(2) and C(4) can adopt ϕ angles of 45° simultaneously, for an axial ligand with Ω = 75° a single ϕ = 45° would place the other ϕ at 27°, and may be expected to produce some strain. In the arrangement seen in H93G Mb, the observed ϕ_1,ϕ_2 pair is very nearly that which minimizes the deflection of any one ϕ value toward an unfavorable value (36.5° and 53.5°, given an Ω of 75°).

[6] The rotation of the imidazole molecule could be influenced partly by the bonding network seen for H93G Mb between the imidazole N_δ and the hydroxyl of Ser-92 and the heme propionate.

ACKNOWLEDGMENT

Mic Feese is thanked for his excellent instruction, assistance, and expertise at every stage of the crystallographic analysis and for his extremely generous gift of time. I also thank R. L. Baldwin for support and suggestions; J. Remington for help and advice in x-ray structure determination; S. G. Boxer, G. DePillis, S. Decatur, and M. Cocco for suggestions and stimulating discussion; M. S. Kay and C. A. Rohl for assistance with DNA sequencing; A. de la Cruz for artwork; and F. W. Dahlquist, S. Baxter, and D. Andrew for careful reading of the manuscript.

REFERENCES

Adachi, S.-i., Nagano, S., Watanabe, Y., Ishimori, K., & Morishima, I. (1991) *Biochem. Biophys. Res. Commun. 180*, 138–144.

Adachi, S.-i., Nagano, S., Ishimori, K., Watanabe, Y., Morishima, I., Egawa, T., Kitagawa, T., & Makino, R. (1993) *Biochemistry 32*, 241–252.

Antonini, E., & Brunori, M. (1971) *Hemoglobin and Myoglobin in their Reactions with Ligands*, North-Holland Publishing Company, Amsterdam, London.

Barrick, D., & Baldwin, R. L. (1993) *Biochemistry 32*, 3790–3796.

Barrick, D., Hughson, F. M., & Baldwin, R. L. (1993) *J. Mol. Biol.* (in press).

Berry, E. A., & Trumpower, B. L. (1987) *Anal. Biochem. 161*, 1–15.

Bren, K. L., & Gray, H. B. (1993) *J. Am. Chem. Soc. 115*, 10382–10383.

Collins, D. M., Countryman, R., & Hoard, J. L. (1972) *J. Am. Chem. Soc. 94*, 2066–2072.

Collman, J. P., Zhang, X., Lee, V. J., Uffelman, E. S., & Brauman, J. I. (1993) *Science 261*, 1404–1411.

den Blaauwen, T., & Canters, G. W. (1993) *J. Am. Chem. Soc. 115*, 1121–1129.

Diven, W. F., Goldsack, D. E., & Alberty, R. A. (1965) *J. Biol. Chem. 240*, 2437–2441.

Dunford, H. B., & Stillman, J. S. (1976) *Coord. Chem. Rev. 19*, 187–251.

Egeberg, K. D., Springer, B. A., Martinis, S. A., Sligar, S. G., Morikis, D., & Champion, P. M. (1990) *Biochemistry 29*, 9783–9791.

Hoard, J. L. (1968) Some Aspects of Heme Stereochemistry, in *Structural Chemistry and Molecular Biology* (Rich, A., & Davidson, N., Eds.) pp 573–594, Freeman, San Francisco.

Hoard, J. L. (1975) Stereochemistry of Porphyrins and Metalloporphyrins, in *Porphyrins and Metalloporphyrins* (Smith, K., Ed.) Elsevier Scientific Publishing Company, Amsterdam.

Hoffman, K. (1953) *Imidazole and its Derivatives*, Part I, Interscience, New York.

Hughson, F. M., Barrick, D., & Baldwin, R. L. (1991) *Biochemistry 30*, 4113–4118.

Kendrew, J. C. (1962) *Brookhaven Symp. Biol. 15*, 216–228.

Laemmli, U. K. (1970) *Nature 227*, 680–685.

Lionetti, C., Guanziroli, M. G., Frigerio, F., Ascenzi, P., & Bolognesi, M. (1991) *J. Mol. Biol. 217*, 409–412.

McLachlan, A. D. (1979) *J. Mol. Biol. 128*, 49–79.

Merino, F., Osuna, J., Bolivar, F., & Soberon, X. (1992) *Biotechniques 12*, 508–509.

Ortiz de Montellano, P. R. (1986) *Cytochrome P-450: Structure, Mechanism, and Biochemistry*, Plenum Press, New York.

Pauling, L. (1960) *Nature of the Chemical Bond*, 3rd ed., Cornell University Press, Ithaca, NY.

Perutz, M. F. (1970) *Nature 228*, 726–734.

Perutz, M. F. (1990) *Mechanisms of Cooperativity and Allosteric Regulation in Proteins*, Cambridge University Press, Cambridge.

Perutz, M. F., Muirhead, H., Cox, J. M., & Goaman, L. C. G. (1968) *Nature 219*, 131–139.

Reynolds, W. F., Peat, I. R., Freedman, M. H., & Lyerla, J. R., Jr. (1973) *J. Am. Chem. Soc. 95*, 328–331.

Rossman, M. G., Ed. (1972) *The Molecular Replacement Method*, Gordon and Breach, New York.

Sanger, F. (1981) *Science 214*, 1205–1210.

Scheler, W., Schoffa, G., & Jung, F. (1957) *Biochem. Z. 329*, 232–246.

Springer, B. A., & Sligar, S. G. (1987) *Proc. Natl. Acad. Sci. U.S.A. 84*, 8961–8965.

Takano, T. (1977) *J. Mol. Biol. 110*, 537–568.

Traylor, T. G., & Scharma, V. S. (1992) *Biochemistry 31*, 2847–2849.

Tronrud, D. E., Ten Eyck, L. F., & Matthews, B. W. (1987) *Acta Crystallogr. A43*, 489–501.

Watson, H. C. (1969) *Prog. Stereochem. 4*, 299–333.

White, D. K., Cannon, J. B., & Traylor, T. G. (1979) *J. Am. Chem. Soc. 101*, 2443–2454.

Zhang, C. (1992) Use of Polyalanine Mutagenesis to Probe the Structure of T4 Lysozyme, Ph.D. Thesis, University of Oregon.